Journal of Mechanical Science and Technology 26 (9) (2012) 2705~2710
www.springerlink.com/content/1738-494x
DOI 10.1007/s12206-012-0715-x

A new method for polygon effect analysis of saw chain †

Shaoqing Shi[1], Xiongqi Peng[2,*], Ning Zhao[3] and Chunwen Zhang[3]

[1]*Department of Civil Engineering, Logistical Engineering University, Chongqing 401311, China*
[2]*School of Materials Science and Engineering, Shanghai Jiao Tong University, Shanghai 200030, China*
[3]*School of Mechanical Engineering, Northwestern Polytechnical University, Xi'an 710072, China*

(Manuscript Received January 4, 2012; Revised April 25, 2012; Accepted May 10, 2012)

Abstract

The polygon effect is a major factor affecting the dynamic characteristics of chain drive in oil saw chain system. It causes impact, noise and dithering of the saw chain and significantly affects the lifespan of oil saw. A simple analytical method is proposed for analyzing the dynamic response resulting from the polygon effect of an oil saw chain system by using the difference method for numerical approximation. A MATLAB program is implemented and then applied for the polygon effect analysis of a specific saw chain drive. Numerical results such as velocities and dynamic loads due to polygon effect are compared with experimental data to demonstrate the effectiveness of the new method. A good agreement is obtained. The proposed polygon effect analysis method can provide guidelines for oil saw chain design for better dynamic performance.

Keywords: Difference method; Dynamics; Polygon effect; Saw chain

1. Introduction

The oil saw is widely used for logging in the forest industry. As a main constitutive part of oil saw, saw chain exhibits traditional problems as so-called polygonal action [1-3]. Differing from the roller chain generally applied in power transmission, the saw chain consists of drive links, tie straps, and cutters, as shown in Fig. 1. The chain forms into a polygon around the sprockets when engaging with the sprockets, leading to velocity variation in the tight and loose sides of the saw chain drive even with a constant revolution speed of the driving sprocket. These velocity oscillations cause accelerations, thus resulting in dynamic loads, noise emission and wear of the saw chain. These problems significantly affect the cutting efficiency and fatigue life of the oil saw.

Polygonal action of the chain drive has been extensively studied during the past decades. Due to the complexity of a chain drive system, many analytical models have been developed for the dynamic analysis of roller chain drives including polygon effect. By separating longitudinal vibration from transverse one, Fawcett and Nicol [4] developed a model for the dynamic analysis on a roller chain drive under constant speed and load. The model took into account the elasticity of the chain and roller-tooth contact. By treating the chain as a traveling uniform heavy string, Ariaratnam and Asokanthan [5] investigated the dynamic instability of chain drives due to polygonal actions. Chen and Freudenstein [6] developed a kinematic analysis model for the motion of roller chain drive. Their results revealed that the center distance has a significant effect on chain performance. Veikos and Freudenstein [7] also investigated the effects of some important factors including impact, and chain elasticity on chain dynamic behavior by using a computer-aided procedure for general application. Peng and Carpino [8] proposed a method for the optimal design of constant velocity chain systems by incorporating the dynamic and kinematic effects of drive links and using a direct perturbation solution for small amplitude oscillations. Srnik and Pfeiffer [9] investigated the dynamics of continuously variable transmissions characterized from the polygonal action of discrete chains. Chain links were modeled as strands with joint forces. Pulleys were described as elastic multibodies to

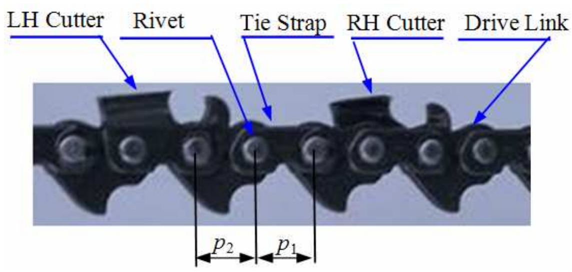

Fig. 1. Saw chain structure.

*Corresponding author. Tel.: +86 21 62813430, Fax.: +86 21 62826575
E-mail address: xqpeng@sjtu.edu.cn
† Recommended by Editor Yeon June Kang

take into account the effect of pulley deformation on the dynamic behavior of the chain drive. By taking into account the effects of chain mass, link elasticity, gravitational forces and inertia forces in the chain, Troedsson and Vedmar [10] presented a model for the dynamic analysis of oscillations in chain drives. The position of the chain was determined by geometric analysis and equilibrium condition. Pedersen et al. [11] developed a roller chain drive model by representing the sprockets as rigid bodies and the chain as mass particles and springs-damper assemblies. Guide bars were used as motion delimiter components on the chain strands between the sprockets. Contact between guide-bars and rollers was taken into account. The dynamics of the roller chain drive associated with the polygon effect was effectively represented in the model. With the extension of this model, Pedersen [12] analyzed contacts between rollers and sprockets in chain-drive systems. The effect of tooth profile was investigated and a real tooth profile was proven to be superior to an idealized circular tooth profile. Except for analytical models, a numerical model based on finite element method was also developed for polygon effect analysis of a chain drive [13].

There is very limited research on the polygon effect of saw chain. By modeling the chain saw as a rigid body and relating it to engine, clutch and flywheel, Reynolds and Soedel [14] presented an analytical model to describe the dynamic characteristics of a non-isolated chain saw. They predicted the acceleration spectra with respect to chain saw operation speeds. Heisel and Schneider [15] presented a method for preventing the polygonal action in saw chain drives by introducing a guide for the chain and acting as a disc cam mechanism.

In this paper, a simple analytical method is proposed for analyzing the dynamic response resulting from the polygon effect of oil saw chain system by using difference method for numerical approximation. A MATLAB program is implemented accordingly. Numerical results such as velocities and dynamic loads due to polygon effect for a specific saw chain are compared with experimental data to demonstrate the effectiveness of the proposed model.

2. Model of oil saw

2.1 System simplifications

For convenience and generality, some simplifications as follows are made for the oil saw shown in Fig. 2:

(1) With the existence of a guide bar in the oil saw, the tight and slack sides are simplified as straight lines, and the motion curves of the saw chain are simplified to four straight lines and two arcs.

(2) Machining error and assembling clearance between hinge pins and drive links and tie straps are neglected.

(3) RH and LH Cutters, which have the same pitch as tie straps, are simplified as tie straps.

(4) Two hinge pins and two link chips are riveted into one tie strap and thus are simplified as one part.

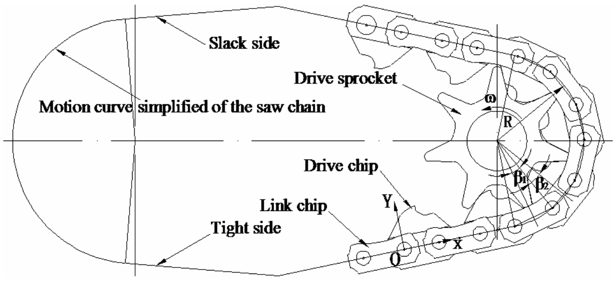

Fig. 2. Simplification of chain saw.

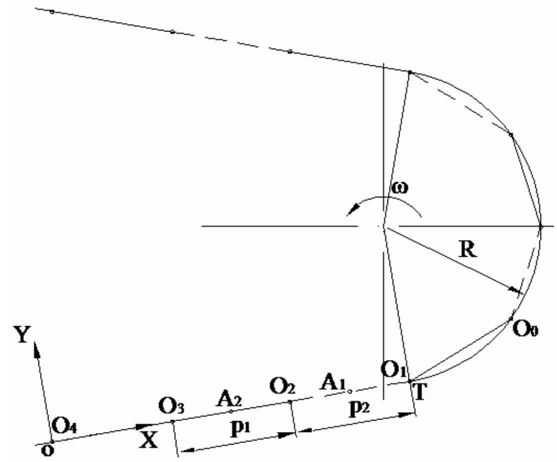

Fig. 3. Schematic for coordinate system and initial positions.

2.2 Geometric conditions for meshing

For stable and reliable meshing between the saw chain and sprocket, the following conditions should be satisfied:

(1) In the stable meshing zone, the centers of hinge pins should be located on the pitch circle of sprockets.

(2) For other zones, the centers of hinge pins are either located on the straight lines of the tight or slack sides or on the pitch circle of sprockets.

(3) The addendum angle of saw chain drive links should be the same as that of sprockets so that face-face contact between sprocket tooth and drive links can be achieved in the stable meshing zone.

2.3 Initial coordinates of critical points

As shown in Fig. 1, the RH and LH cutters are simplified as tie straps. The drive links and tie straps are modeled as rigid trusses with center of gravity located at the midpoint of the trusses. The pitch radius of the sprocket varies with the pitches of the drive link and tie straps and can be calculated as

$$R = \frac{\sqrt{p_1^2 + p_2^2 + 2p_1p_2\cos\left(\pi/z\right)}}{2\sin\left(\pi/z\right)} \tag{1}$$

where R is the pitch radius of the sprocket, z is number of teeth of the sprocket, p_1 and p_2 are the pitches of the drive links and tie straps, respectively.

As shown in Fig. 3, take one drive link (O_1O_2) and its neighboring tie strap (O_2O_3) as a unit for polygon effect analysis.

Assume that the hinge joints O_1, O_2, O_3 and O_4 are located at the tight side, which is the tangent of the sprocket pitch circle. At the initial time, point O_1 coincides with the tangent point T, as shown in Fig. 3. A local stationary coordinate system XOY, in which the coordinate origin coincides with O_4 at the initial time and the local x-axis is along the tight side, is set up for polygon effect analysis with difference method.

In the stationary local coordinate system XOY, the coordinates of point T are

$$T_x = p_1 + 2p_2, \quad T_y = 0 . \tag{2}$$

The initial coordinates of point O_2 and O_3 are:

$$\begin{cases} O_{2x}^0 = p_1 + p_2 \\ O_{2y}^0 = 0 \end{cases}, \qquad \begin{cases} O_{3x}^0 = p_2 \\ O_{3y}^0 = 0 \end{cases}. \tag{3}$$

Suppose that A_1 and A_2 are the midpoints of O_1O_2 and O_2O_3, respectively, as shown in Fig. 3, then the initial coordinates of A_1 and A_2 are:

$$\begin{cases} A_{1x}^0 = p_1 + \frac{3}{2} p_2 \\ A_{1y}^0 = 0 \end{cases}, \qquad \begin{cases} A_{2x}^0 = \frac{1}{2} p_1 + p_2 \\ A_{2y}^0 = 0 \end{cases}. \tag{4}$$

3. Dynamics analysis of polygon effect of saw chain

3.1 Time period division

Suppose that after the sprocket rotates counterclockwise for t_1 seconds, O_2 just reaches to T, then,

$$\omega t_1 = 2\arcsin\left(\frac{p_2}{2R}\right). \tag{5}$$

After the sprocket rotates counterclockwise for t_2 seconds, O_3 just reaches to T, then

$$\omega t_2 = 2\arcsin\left(\frac{p_1}{2R}\right) + 2\arcsin\left(\frac{p_2}{2R}\right). \tag{6}$$

Thus, in one period, the dynamic analysis for polygon effect of saw chain system can be divided into two stages:

(1) $t \in (0, t_1]$: O_1 enters the pitch circle trajectory of the sprocket, while O_2 is still located on the tight side line track.

(2) $t \in (t_1, t_2]$: O_2 enters the pitch circle trajectory of the sprocket, while O_3 is still located on the tight side line track.

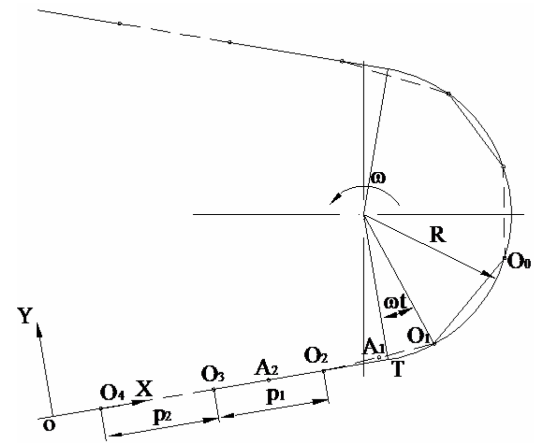

Fig. 4. Sprocket rotating t seconds from initial position in Fig. 3.

3.2 Real-time coordinates of key points

With the sprocket rotating counterclockwise for t seconds, as shown in Fig. 4, the real-time coordinates for each key point are derived as follows:

(1) $0 < t \le t_1$.

During this time interval, O_1 enters the pitch circle trajectory of the sprocket while O_2 is still located on the tight side line track. The tie strap translates along the tight side. The real-time coordinates of points O_1 and O_2 satisfy the following equations:

$$\begin{cases} O_{1x} = p_1 + 2p_2 + R\sin\omega t \\ O_{1y} = R - R\cos\omega t \\ \left(O_{1x} - O_{2x}\right)^2 + O_{1y}^2 = p_2^2 \\ O_{2y} = 0 \end{cases}. \tag{7}$$

The real-time coordinates of midpoint A_1 are given by:

$$A_{1x} = \frac{1}{2}\left(O_{1x} + O_{2x}\right), \quad A_{1y} = \frac{1}{2}\left(O_{1y} + O_{2y}\right). \tag{8}$$

(2) $t_1 < t \le t_2$.

During this time interval, O_2 enters the pitch circle trajectory of the sprocket while O_3 is still located on the tight side line track. The drive link O_1O_2 enters the stable meshing zone. No relative motion happens between the drive link O_1O_2 and the sprocket, so no polygon effect appears for the drive link O_1O_2. The real time coordinates of points O_2 and O_3 satisfy the following equations:

$$\begin{cases} O_{2x} = p_1 + 2p_2 + R\sin\omega\left(t - t_1\right) \\ O_{2y} = R - R\cos\omega\left(t - t_1\right) \\ \left(O_{2x} - O_{3x}\right)^2 + O_{2y}^2 = p_1^2 \\ O_{3y} = 0 \end{cases}. \tag{9}$$

The real-time coordinates of midpoint A_2 are given by:

$$A_{2x} = \frac{1}{2}\left(O_{2x} + O_{3x}\right), \quad A_{2y} = \frac{1}{2}\left(O_{2y} + O_{3y}\right). \tag{10}$$

3.3 Polygon effect analysis for one period

(1) $0 < t \le t_1$.

Suppose that $\vec{U}_{A_1}$ and $\vec{U}_{O_2}$ are the displacements of points A_1 and O_2, respectively, at time t ($0 < t \le t_1$),

$$\vec{U}_{A_1} = \vec{A}_1 - \vec{A}_1^0, \quad \vec{U}_{O_2} = \vec{O}_2 - \vec{O}_2^0 \tag{11}$$

where $\vec{A}_1$ is the current position vector of point A_1 defined by Eq. (8), $\vec{A}_1^0$ is the original position vector of point A_1 defined by Eq. (4). $\vec{O}_2$ and $\vec{O}_2^0$ are position vectors defined in a similar way by Eqs. (3) and (7), respectively.

By dividing t_1 into K parts, the velocities of points A_1 and O_2, $\vec{V}_{A_1}$ and $\vec{V}_{O_2}$, respectively, can be obtained by difference method as a numerical approximation:

$$\vec{V}_{A_1}^{i\Delta t} = \frac{\vec{U}_{A_1}^{i\Delta t} - \vec{U}_{A_1}^{(i-1)\Delta t}}{\Delta t}, \quad \vec{V}_{O_2}^{i\Delta t} = \frac{\vec{U}_{O_2}^{i\Delta t} - \vec{U}_{O_2}^{(i-1)\Delta t}}{\Delta t} \tag{12}$$

where $i = 1, \cdots, K$. The initial velocities of points A_1 and O_2 are both $\vec{V}^0 = \begin{Bmatrix} R\omega \\ 0 \end{Bmatrix}$, and the initial displacements of points A_1 and O_2 are both $\vec{U}^0 = \begin{Bmatrix} 0 \\ 0 \end{Bmatrix}$.

Similarly, the accelerations of points A_1 and O_2, $\vec{a}_{A_1}$ and $\vec{a}_{O_2}$, respectively, are:

$$\vec{a}_{A_1}^{i\Delta t} = \frac{\vec{V}_{A_1}^{i\Delta t} - \vec{V}_{A_1}^{(i-1)\Delta t}}{\Delta t}, \quad \vec{a}_{O_2}^{i\Delta t} = \frac{\vec{V}_{O_2}^{i\Delta t} - \vec{V}_{O_2}^{(i-1)\Delta t}}{\Delta t} \tag{13}$$

where $i = 1, \cdots, K$. The initial accelerations of points A_1 and O_2 are both $\vec{a}^0 = \begin{Bmatrix} 0 \\ 0 \end{Bmatrix}$.

The dynamic load of A_1 resulting from the polygon effect in the drive link is:

$$F_{dA_1x} = m_C a_{A_1x}, \qquad F_{dA_1y} = m_C a_{A_1y} \tag{14}$$

where m_C is the mass of the drive link.

In the time interval $0 < t \le t_1$, the tie straps and drive links after point O_2 will translate along the x-axis on the tight side of the saw chain. They will have the same acceleration as point O_2. Hence, the dynamic load on the tight side tie straps and drive links after point O_2 is:

$$F_{dO_2x}^L = m_L a_{O_2x}, \quad F_{dO_2x}^C = m_C a_{O_2x} \tag{15}$$

where m_L and m_C are the mass of tie strap and drive link, respectively.

The total dynamic load on the tight side of the saw chain due to polygon effect is:

$$F_{dx} = F_{dA_1x} + MF_{dO_2x}^L + NF_{dO_2x}^C, \qquad F_{dy} = F_{dA_1y} \tag{16}$$

where M and N are the number of tie straps and drive links of the tight side of the saw chain after point O_2, respectively.

(2) $t_1 < t \le t_2$.

Suppose that $\vec{U}_{A_2}$ and $\vec{U}_{O_3}$ are the displacements of points A_2 and O_3, respectively, at time t ($t_1 < t \le t_2$),

$$\vec{U}_{A_2} = \vec{A}_2 - \vec{A}_2^0, \quad \vec{U}_{O_3} = \vec{O}_3 - \vec{O}_3^0 . \tag{17}$$

By dividing $t_2 - t_1$ into K parts, the velocities of points A_2 and O_3, $\vec{V}_{A_2}$ and $\vec{V}_{O_3}$, respectively, can be obtained by difference method as a numerical approximation:

$$\vec{V}_{A_2}^{i\Delta t} = \frac{\vec{U}_{A_2}^{i\Delta t} - \vec{U}_{A_2}^{(i-1)\Delta t}}{\Delta t}, \quad \vec{V}_{O_3}^{i\Delta t} = \frac{\vec{U}_{O_3}^{i\Delta t} - \vec{U}_{O_3}^{(i-1)\Delta t}}{\Delta t} \tag{18}$$

where $i = 1, \cdots, K$. At $t = t_1$, the velocities of points A_2 and O_3 are both $\vec{V}_1 = \vec{V}_{O_2}^{t_1}$, and the initial displacements of points A_2 and O_3 are both $\vec{U}_1 = \vec{U}_{O_2}^{t_1}$.

Accordingly, the accelerations of points A_2 and O_3, $\vec{a}_{A_2}$ and $\vec{a}_{O_3}$, respectively, are:

$$\vec{a}_{A_2}^{i\Delta t} = \frac{\vec{V}_{A_2}^{i\Delta t} - \vec{V}_{A_2}^{(i-1)\Delta t}}{\Delta t}, \quad \vec{a}_{O_3}^{i\Delta t} = \frac{\vec{V}_{O_3}^{i\Delta t} - \vec{V}_{O_3}^{(i-1)\Delta t}}{\Delta t} \tag{19}$$

where $i = 1, \cdots, K$. At $t = t_1$, the accelerations of points A_2 and O_3, are both $\vec{a}_1 = \vec{a}_{O_2}^{t_1}$.

The dynamic load of A_2 resulting from the polygon effect in the tie strap is:

$$F_{dA_2x} = m_L a_{A_2x}, \quad F_{dA_2y} = m_L a_{A_2y} \tag{20}$$

where m_L is the mass of the tie strap.

In the time interval $t_1 < t \le t_2$, the tie straps and drive links after point O_3 will translate along the x-axis on the tight side of the saw chain. They will have the same acceleration as point O_3. Hence, the dynamic load on the tight side tie straps and drive links after point O_3 is:

$$F_{dO_3x}^L = m_L a_{O_3x}, \quad F_{dO_3x}^C = m_C a_{O_3x} . \tag{21}$$

The total dynamic load on the tight side of the saw chain due to polygon effect is:

$$F_{dx} = F_{dA_2x} + MF_{dO_3x}^L + NF_{dO_3x}^C, \qquad F_{dy} = F_{dA_2y} \tag{22}$$

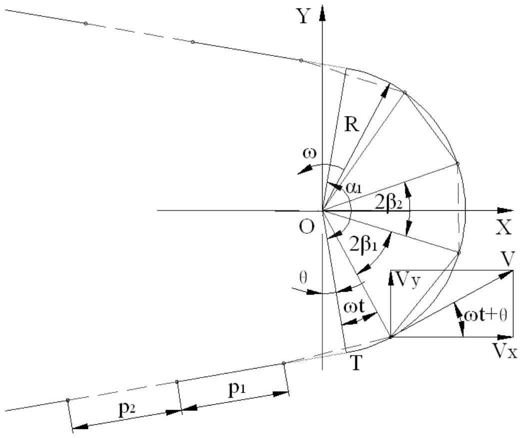

Fig. 5. Schematic for traditional method for polygon effect analysis.

where M and N are the number of tie straps and drive links of the tight side of the saw chain after point O_3, respectively.

3.4 Polygon effect analysis in reference

According to the dynamics analysis theory on polygon effect of chain drive in textbook for machine design [16], taking the drive link as the analysis object, as shown in Fig. 5, the horizontal velocity, acceleration and dynamic load of the drive link is:

$$\begin{cases} V_x^C = R\omega\cos(\omega t+\theta) \\ a_x^C = \dfrac{dV_x^C}{dt} = -R\omega^2\sin(\omega t+\theta) \\ F_{dx}^C = m_x^C a_x^C \ . \end{cases} \tag{23}$$

4. Numerical results and discussion

The proposed numerical method for polygon effect analysis is demonstrated on a typical oil saw chain with the following parameters: tie strap pitch $p_1 = 8.91\,mm$, drive link pitch $p_2 = 7.56\,mm$, number of sprocket teeth $z = 8$, number of tie straps (M) and drive links (N) of the tight side $M = N = 32$, mass of tie strap $m_L = 1.906\,g$, mass of drive link $m_C = 1.296\,g$, rotational speed of the sprocket $\omega = 6550$ $r/\min$.

Fig. 6 shows the testing system for an oil saw. The above saw chain is tested under unloaded condition and its velocity of the tight side in one period ($0 < t \le t_2$) is recorded and shown in Fig. 7 with squares. The velocity of the tight side predicted by the proposed method is plotted in Fig. 7 by a solid line. As comparison, the velocity of the tight side predicted from [16] is shown in Fig. 7 by a dashed line. As shown in Fig. 7, the velocity measured is about $14.6\,m/s$ with a fluctuation of $0.2\,m/s$. The velocity predicted by the proposed model is about $14.57 \sim 14.77\,m/s$, which is in a good agreement with testing data. In contrast, the velocity predicted from Ref. [16] deviates considerably from the testing data.

Fig. 6. Saw chain testing system.

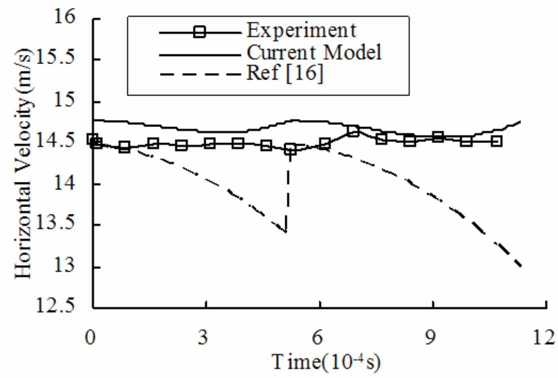

Fig. 7. The tight side velocity of the saw chain.

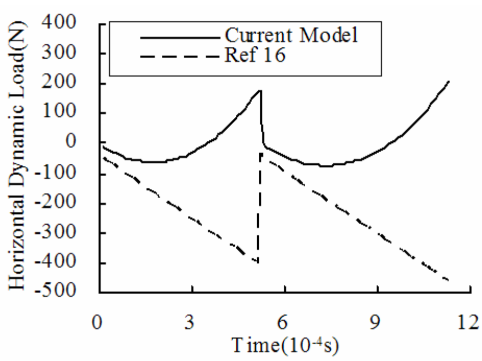

Fig. 8. The total tight side dynamic loads of the saw chain.

The predicted total dynamic loads on the tight side due to polygon effect are shown in Fig. 8. The dynamic load predicted by the proposed model is in the range of $-74.5 \sim 209.4N$ compared to $-33.4 \sim -463.2N$ from Ref. [16], as shown in Fig. 8.

Obviously, Ref. [16] predicts an unrealistic dynamic load, as the oil saw may operate under a rotational speed as high as 12000 r/min, which implies a nearly 1000N dynamic load. In fact, the load predicted from Ref. [16] with Eq. (23) is only centrifugal force existing in all circular motion, not from the polygon effect.

5. Conclusions

Based on kinematic analysis and by using difference method for numerical approximation, a very simple and effective analytical model is developed for dynamics analysis on polygon effect of oil saw chain system and is demonstrated on a specific saw chain. The results show good agreement with experimental data and indicate some general trends, which provide additional insight into the dynamic behavior of the saw chain system resulting from polygonal action. The proposed analytical method provides a solid foundation for the optimal design of saw chain and fatigue life evaluation of the saw chain system.

Acknowledgment

This work is supported by the National Natural Science Foundation of China (50975236, 11172171).

References

[1] R. A. Morrison, Polygonal action in chain drives, *Machine Design*, 24 (1952) 155-159.
[2] S. Mahalingam, Polygonal action in chain drives, *Journal of the Franklin Institute*, 265 (1) (1958) 23-28.
[3] G. Bouillon and G. V. Tordion, On polygonal action in roller-chain drives, *Journal of Engineering for Industry-Transactions of the ASME*, 87 (1965) 243-250.
[4] J. N. Fawcett and S. W. Nicol, Vibration of a roller chain drive operating at constant speed and load, *Proceedings of the Institution of Mechanical Engineers*, 194 (1) (1980) 97-101.
[5] S. T. Ariaratnam and S. F. Asokanthan, Dynamic stability of chain drives, *Journal of Mechanisms, Transmissions, and Automation in Design*, 109 (3) (1987) 412-418.
[6] C. K. Chen and F. Freudenstein, Toward a more exact kinematics of roller chain drives, *ASME Journal of Mechanisms, Transmissions and Automation in Design*, 110 (3) (1988) 269-275.
[7] N. M. Veikos and F. Freudenstein, On the dynamic analysis of roller chain drives, *Mechanical Design and Synthesis ASME*, 46 (1992) 431-450.
[8] J. P. Peng and M. Carpino, Optimal design of the path of chain link systems, *Journal of Mechanical Design, Transactions of the ASME*, 115 (4) (1993) 793-799.
[9] J. Srnik and F. Pfeiffer, Dynamics of CVT chain drives, *International Journal of Vehicle Design*, 22 (1) (1999) 54-72.
[10] I. Troedsson and L. Vedmar, A dynamic analysis of the oscillations in a chain drive, *Journal of Mechanical Design*, 123 (3) (2001) 395-401.
[11] S. L. Pedersen, J. M. Hansen and A. C. Ambrósio, A roller chain drive model including contact with guide-bars, *Multibody System Dynamics*, 12 (3) (2004) 285-301.
[12] S. L. Pedersen, Model of contact between rollers and sprockets in chain-drive systems, *Archive of Applied Mechanics*, 74 (7) (2005) 489-508.
[13] H. Zheng, Y. Y. Wang and K. P. Quek, A refined numerical simulation on dynamic behavior of roller chain drives, *Shock and Vibrat*ion, 11 (5) (2004) 573-584.
[14] D. D. Reynolds and W. Soedel, Analytical vibration analysis of non-isolated chain saws, *Journal of Sound and Vibration*, 44 (4) (1976) 513-523.
[15] U. Heisel and M. Schneider, Prevention of chordal action in chain drives as feed systems in through feed machining of wooden panels, *Proceedings of the 19th International Wood Machining Seminar*, China (2009) 113-121.
[16] L. G. Pu and M. G. Ji, *Machine design*, Higher Education Press, Beijing, China (2001).

Shaoqing Shi received his B.E. in Oil Storage and Transportation from Logistical Engineering University, China in 1987, and Ph.D. in General Mechanics in 1998 from Northwestern Polytechnical University, China. He is currently a professor and head of Civil Engineering, Logistical Engineering University. His main research interests are dynamical analysis, reliability and vibration control. He is the director of China Association for Engineering Construction Standardization and member of the Chinese Society of Theoretical and Applied Mechanics. His recent research about explosion shock wave and antiknock technology has been awarded second prize in Natural Science of Chongqing.

Xiongqi Peng received his Ph.D. in Mechanical Engineering from Northwestern University, USA, in 2003. He is currently a professor at the School of Materials Science and Engineering in Shanghai Jiao Tong University, China. His main research interests include computational mechanics, finite element method, and composite materials.